ANALYSIS OF THE CHLORIDE BINDING ABILITY OF CEMENTS

Károly Kovács, Jolán Csizmadia and György Balázs

Department of Building Materials
Technical University of Budapest
H–1521 Budapest, Hungary

Received: March 4, 1997

Abstract

We examined the binding process of NaCl penetrating into hardened cements from outer source through Hungarian manufactured cements representing both general and special fields of application. These types are the following: 450 Rpc, S 54, 350 ppc 20 and 250 kspc 60. We observed the effect of chlorides entering cements (between 1–28 and 28–56 days) by thermal analysis and X-ray diffraction spectroscopy. X-ray diffraction analysis proved that the chloride ion of NaCl is bound by C_3A and C_4AF in the form $C_3A \cdot CaCl_2 \cdot H_{10}$ and the analogous $C_3F \cdot CaCl_2 \cdot H_{10}$ containing ferrite. Chloro-aluminate-hydrates were formed not only in the first phase of hydration but in the hardened cement as well by the substitution of anions of the present AF_m phases: $C_3A \cdot CaSO_4 \cdot H_{12}, C_3A \cdot Ca(OH)_2 \cdot H_{12}, C_3A \cdot CaCO_3 \cdot H_{11}$.

Neither X-ray diffraction nor thermal analysis investigations detected any chlorous calcium-silicate-hydrates.

Keywords: chloride binding, cements.

1. Introduction

Chloride ion may enter concretes in three ways:
- through mineralizators or contamination during the production of cement,
- during the preparation of concrete,
- after the concrete has hardened, for example by road defrostation.
  Chloride ion may appear in cements in the following forms:

a) Chemically bound. Chemically bound chloride does not corrode reinforcement steels.

b) Physically bound, adhering to capillary walls after adsorption. The role of this chloride in corrosion is not yet clear.

c) Dissolved in pore waters free chloride ions are the main cause of the corrosion of reinforcement steels [1, 2].

The proportions of free and bound chlorides may be determined by laboratory analysis. Numerous previous experiments analysed the way how

chloride ions added to cement pastes are bound in clinker minerals and cements. The question whether cements can bind chloride ions penetrating into concretes up to years after the preparation of the concrete came up only after the entry of wintertime road defrostation. The paper discusses this particular process.

According to literature information on chlorides added during the preparation [3, 4] the chloride binding ability of cements is dominated by their composition. Chloride binding capacity is mainly determined by the calcium-aluminates (C_3A, C_4AF) and alkaline (K_2O, Na_2O) content. Calcium-aluminates decrease the chloride ion concentration of pore water by forming $C_3A \cdot CaCl_2 \cdot H_{10}$ and the analogous $C_3F.CaCl_2 \cdot H_{10}$ containing ferrite. Alkalis – though they inhibit the $C_3A + Cl^-$ reaction – increase the hydroxide ion concentration in the pore water. The increased concentration of hydroxide ions [5, 6] decreases the ratio between Cl^-/HO^-; the lower this ratio, the lower the danger of corrosion becomes. The Cl^-/HO^- ratio in cements depends on the pH value and the amount of chloride that the solid phase is able to bind. Only part of free chlorides are bound in the form of $C_3A \cdot CaCl_2 \cdot H_{10}$ [7].

Due to the strong alkaline pH value of cements, an oxide layer appears on the surface of reinforcement steels. The protective effect dies if the concentration of free chlorides initiating corrosion reaches a certain level, or if the concentration of HO^- is so limited that the passivative ferrite-oxide layer becomes unstable.

The concrete's tolerance level is 35% higher when NaCl is present [8] than in the presence of $CaCl_2$ [9]. Carbonatization and outer temperatures above normal decrease the Cl^- binding ability by breaking down chloro-aluminates.

According to relevant literature [10] silicate clinker minerals $(C_3S, \beta C_2S)$ influence the chloride binding process – though they do not bind chlorides chemically.

We tried to identify the role of the different clinkers in the chloride binding process [11] through modelling experiments.

Cement mixtures made from clinkers and gypsum, however, are not merely the mixture of these two ingredients. During the process of cement hydration silicates and aluminates form complicated products, so even the smallest equilibrium disturbances may cause changes in the structure and chemical composition of the product. Even a mixture containing only the fundamental constituents is a multicomponent system itself, as the hydration products of the four basic clinker components that are always or almost always present $(C_3S, C_2S, C_3A, C_4AF)$ form several different products according to the hydration circumstances, that affect each other's base reactions (supporting, blocking or balancing them). The influence of the

added gypsum and all the known processes affecting the permanence of stability of the formed hydrate products (for example balance of ettringite-formation breakdown, etc.) also has to be considered.

Physical structure depending on the circumstances has strong influence on the balance processes [12, 13]. The compactness, the free water content, the absorbed water content of the cement and hydraulic additives have dominant influence too. That is how that particular cement structure is generated where chloride ion is bound partly chemically and partly by secondary, physical bonds.

2. Experimental Details

The analysed Hungarian cement products represented the following four types: rapid Portland cement (450 Rpc), sulphate resistant Portland cement (S 54 350 pc), fly ash Portland cement (350 ppc 20), slag Portland cement (250 kspc 60). These types correspond to the following international standard types:

rapid Portland cement   -   RPC
sulphate resistant pc.   -   SRPC
fly ash pc.   -   PFAPC (pulverized fly ash PC)
slag pc.   -   GGBSPC (ground granulated
                        blast furnace slag PC)

The characteristics of the different cements are summarized in *Table 1*.

A series of experiments shown in *Table 2* were carried out to investigate the chloride binding ability of cements of different compositions.

Both the activity level of hydraulic additives increasing the cement heterogeneity and the effect of grinding fineness on chemical reactions were disregarded.

Cement paste samples of $10 \times 10 \times 50$ mm were prepared for each series; a slice of approx. 1 cm^3 was cut off on the days of the examinations. Derivatogram was recorded for the departed slices, and X-ray diffraction analysis was carried out for each etalon sample, and for each sample stored in saturated salt solution between 1–28 days.

The features of the analytical equipment used are the following:

Derivatograph:
type   MOM Q-1500D
reference material Al_2O_3
sample weight $170 + 20$ mg
crusible   corundum
heating rate 10 °C/min

Table 1
Results of the chemical and physical analysis of cements

Cement sign Cement factory		250 kspc 60 Vác	450 Rpc Vác	S54 350 pc Lábatlan	350 ppc 20 Lábatlan
Chemical composition					
Heating loss		1.13	1.07	1.65	1.50
SiO_2	%	28.54	20.71	20.39	23.58
CaO	%	53.08	63.60	61.16	56.28
MgO	%	2.40	2.09	2.82	3.72
Al_2O_3	%	6.89	5.43	4.76	5.75
Fe_2O_3	%	1.78	3.51	5.12	3.92
SO_3	%	3.11	2.85	2.86	2.55
Insoluble in HCl	%	0.80	0.55	1.21	1.96
Free CaO	%		1.78	0.56	
Mineral composition					
C_3S	%		45.20	45.06	
βC_2S	%		25.69	25.47	
C_3A	%		8.55	4.01	
C_4AF	%		10.80	15.85	
AM	%		1.55	0.93	
Physical characteristics					
density	g/ml	2.997	3.172	3.199	2.912
specific surface area					
(Blaine)	m^2/kg	284	345	329	338
binding water	%	28.7	28.7	23.3	29.0
start of setting		3 h 30 min	2 h 20 min	1 h 10 min	3 h 45 min
end of setting		5 h 45 min	4 h 20 min	3 h 50 min	6 h
remained on sieve					
0.2 mm sieve	%	0.08	0.05	0.4	1.40
0.09 mm sieve	%	1.79	1.25	7.64	10.99
volume permanency		adequate	adequate	adequate	adequate

temperature range   20 − 980 °C
sensibility   0.5 mg/grade
atmosphere   air

X-ray diffractometer:
type   JEOZ JDX 85
X-ray tube   Cu K_α
accelerating voltage   40 kV
anode current strength   40 mA
sensibility 1×10^3 c/s
goniometer speed   2 degrees/min (θ)
paper speed   20 unit/min

Table 2

Analysed cements and hydration circumstances

Sign	Cement type	Mixing water compared to cement	Storing temperature °C	Salt treatment	Relative humidity, % after treatment
1	450 Rpc	k = 0.287	20	1	100
2	450 Rpc	k = 0.287	20	2	100
3	450 Rpc	k = 0.287	20	3	100
4	450 Rpc	k = 0.287	20	4	100
5	S 54 350 pc	k = 0.233	20	1	100
6	S 54 350 pc	k = 0.233	20	2	100
7	S 54 350 pc	k = 0.233	20	3	100
8	S 54 350 pc	k = 0.233	20	4	100
9	350 ppc 20	k = 0.290	20	1	100
10	350 ppc 20	k = 0.290	20	2	100
11	350 ppc 20	k = 0.290	20	3	100
12	350 ppc 20	k = 0.290	20	4	100
13	250 kspc 60	k = 0.287	20	1	100
14	250 kspc 60	k = 0.287	20	2	100
15	250 kspc 60	k = 0.287	20	3	100
16	250 kspc 60	k = 0.287	20	4	100
17	450 Rpc	k = 0.287	20	etalon	100
18	S 54 350 pc	k = 0.233	20	etalon	100
19	350 ppc 20	k = 0.290	20	etalon	100
20	250 kspc 60	k = 0.287	20	etalon	100

Treatment: 1 – 10% NaCl solution between 24 hours and 28 days
2 – saturated NaCl solution between 24 hours and 28 days
3 – 10% NaCl solution between 28 and 56 days
4 – saturated NaCl solution between 28 and 56 days
Date of analysis: The age of 1, 28, 56, 90 and 180 days
Remarking: k = binding water

3. Results and Evaluation

DTG curves of the derivatograms for each 90 day old reference samples stored in 100% relative humidity are of identical nature (*Fig. 1*). Each has 3 main peaks. The peak around 100 °C shows the continuous leaving [14] of different types of the cement's water content (humidity adhering to the surface, interlayer water, pore water, crystal water of AF_m phases and ettringite, water from partial dehydration of C-S-H gel). The shoulder appearing occasionally under 100 °C belongs to surface humidity, the ones around 180 °C and 280 − 300 °C are the effect of AF_m phases: $C_3A \cdot Ca(OH)_2 \cdot H_{12}$, $C_3A \cdot CaSO_4 \cdot H_{12}$. C-S-H gel also loses water around 300 °C. These shoulders and enlarged peaks are of limited intensity, the presence

of AF_m phases is shown rather by the expansion of the peak. Cement type 350 ppc 20 is an exception; the appearance of monophases is significant due to the higher Al_2O_3 content of this particular cement type (*Fig. 2*).
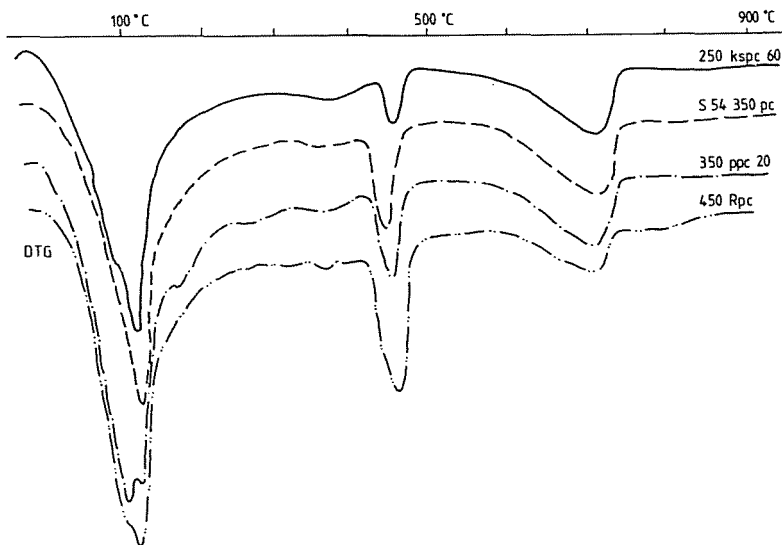
Fig. 1. DTG curves of 90 day old reference hydrated cement samples

Portlandite $\left(Ca(OH)_2\right)$ formed during hydration loses 1 mole water around 460 °C. The degree of hydration may be measured by the weight loss at this peak. *Fig. 1* clearly shows that among the four cement types from 450 Rpc is formed most $Ca(OH)_2$, while 250 kspc 60 and 350 ppc 20 form the lowest amount. This is due to the higher reactivity (450 Rpc) and to the fact that hydraulic additive materials of cements containing slag or fly ash react with portlandite generated from C_3S and C_2S during the hydration of cement, forming secondary C-S-H gel. Numeric results are given in *Tables 3, 4, 5, 6* and *7* in the percentage of the weight of input materials calculated from the TG curves of the derivatograms.

The order of reaction rate of the four different cement types is the following:

$$450 \text{ Rpc} \geq 350 \text{ ppc} \geq 250 \text{ kspc } 60 \geq S54$$

$CaCO_3$ loses 1 mole of CO_2 at the third DTG peak between 600 and 800 °C.

We have to mention the special characteristic of DTG curves bending significantly low over 550 °C (550 − 650 °C) as hydration proceeds. This is the temperature range where C-S-H gel loses its remaining crystal water content.
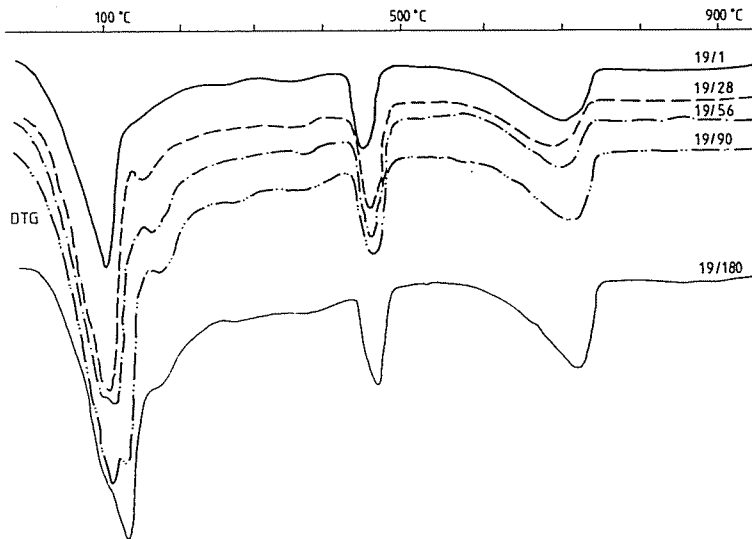
Fig. 2. DTG curves of hydrated cement pastes prepared
of 350 ppc 20 cement at different age
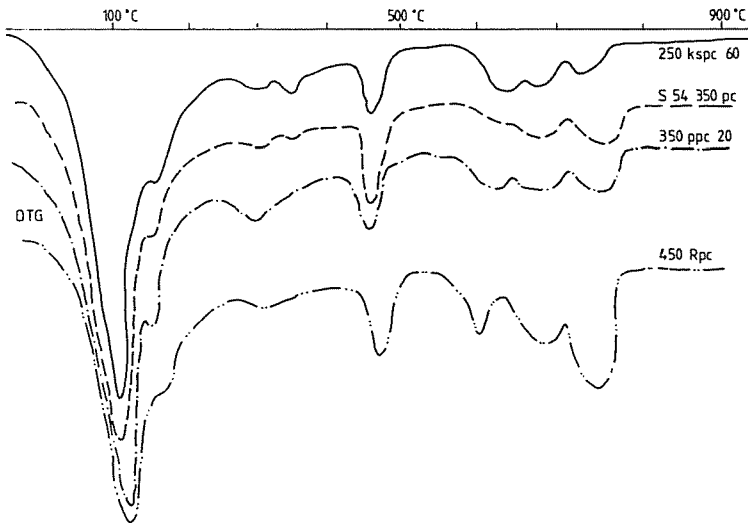
Fig. 3. DTG curves of hydrated cement pastes stored
in saturated NaCl solution between 1-28 days

K. KOVÁCS et al.
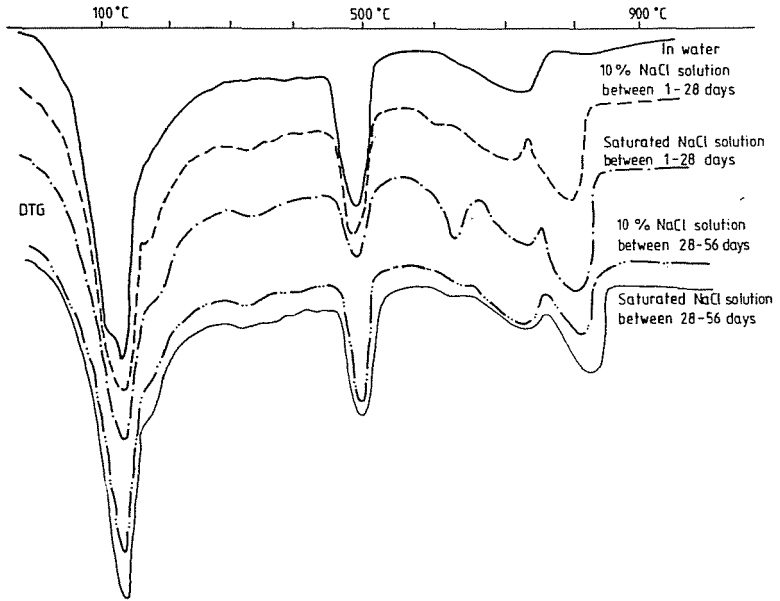
Fig. 4. Influence of salt treatment on the hydration of 90 day old hydrated cement pastes
made of 450 Rpc (according to the DTG curves)
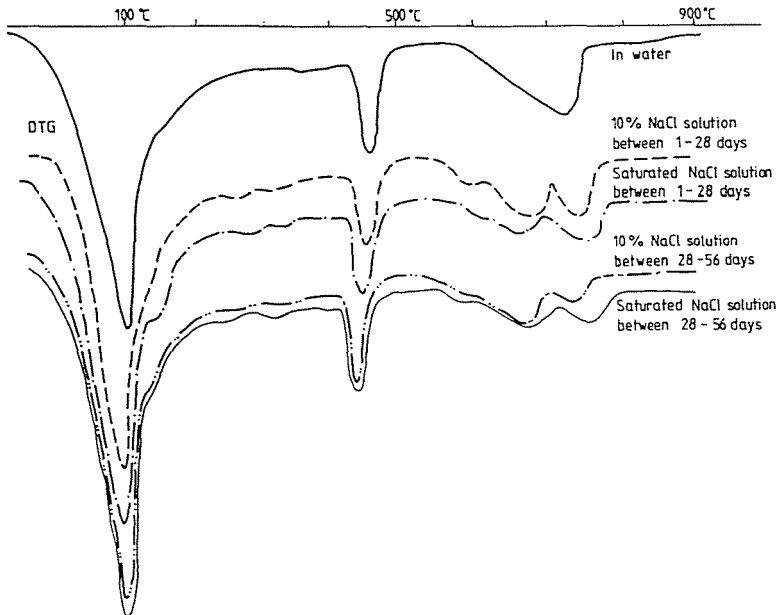
Fig. 5. Influence of salt treatment on the hidration of 90 day old hydrated cement pastes
made of S 54 350 pc (according to the DTG curves)
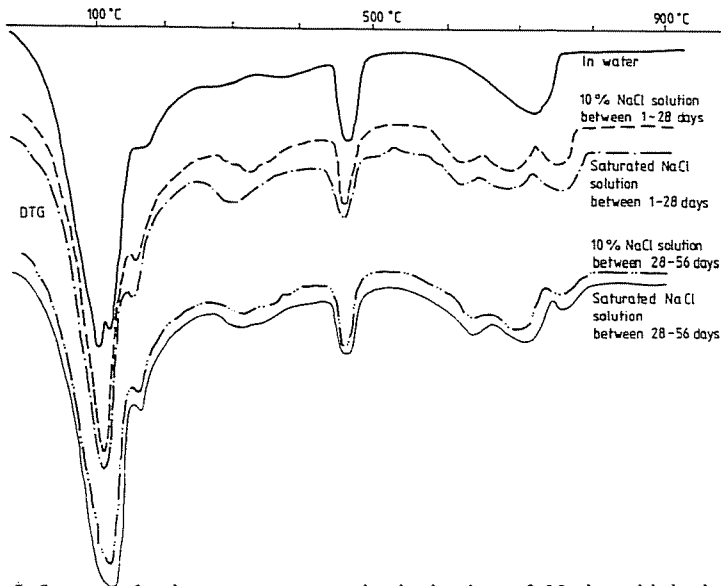
Fig. 6. Influence of salt treatment on the hydration of 90 day old hydrated cement samples made of 350 ppc 20 (according to the DTG curves)
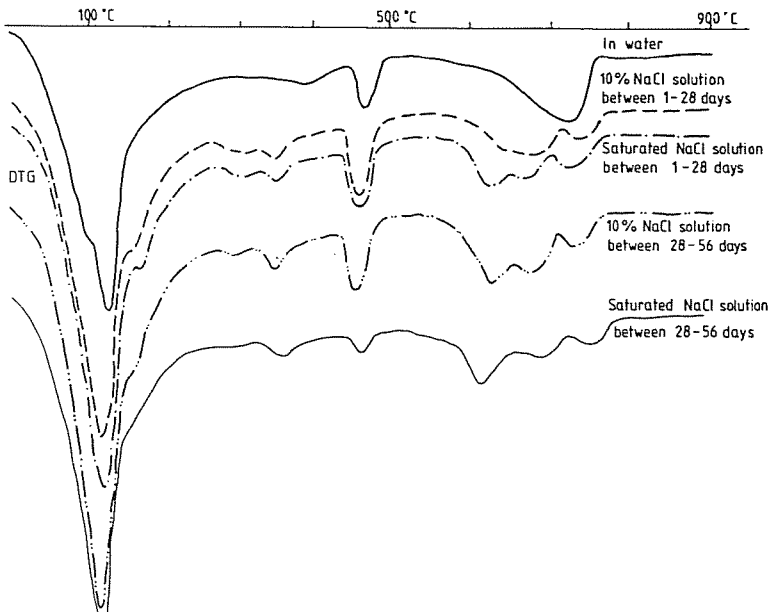
Fig. 7. Influence of salt treatment on the hydration of 90 day old hydrated cement samples made of 350 kspc 60 (according tv the DTG curves)
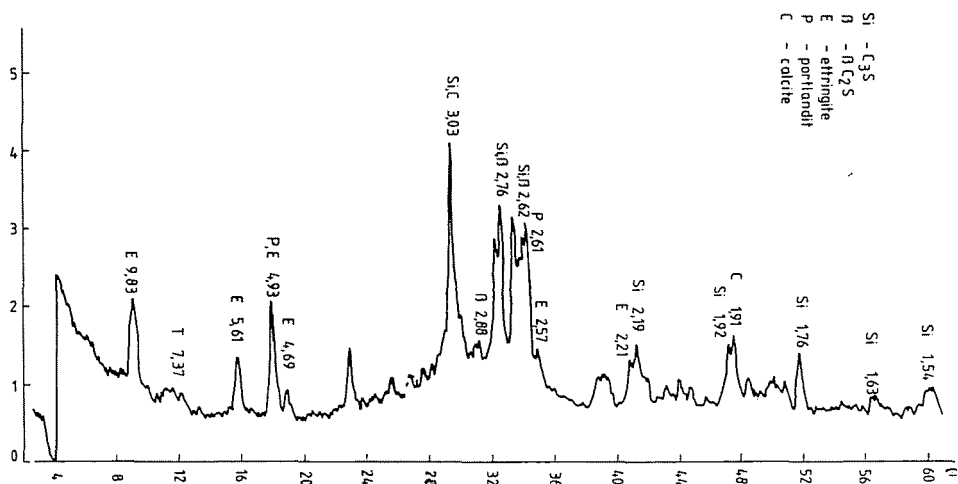
Fig. 8. X-ray diffraction spectrum of 150 day-old 250 kspc 60 cement paste stored in an atmosphere of 100% relative humidity
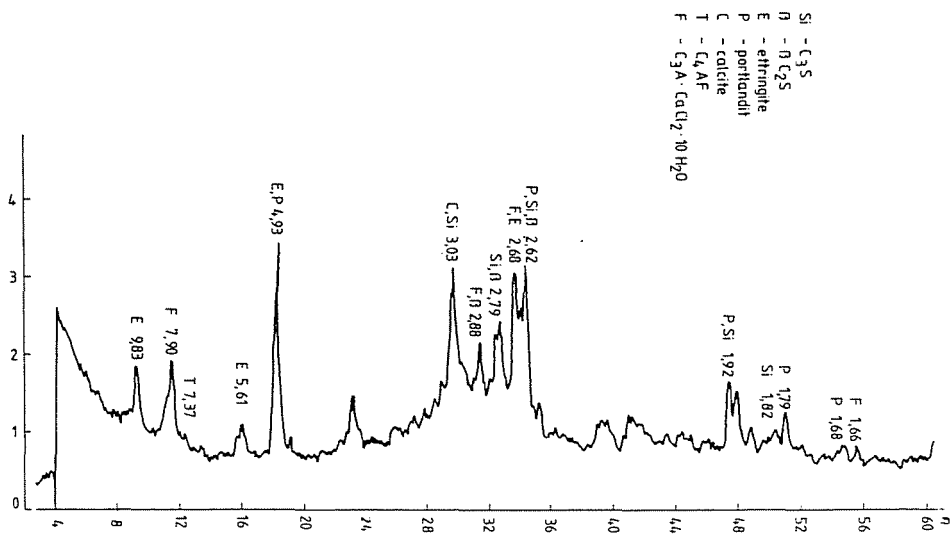
Fig. 9. X-ray diffraction spectrum of hydrated cement sample made of 250 kspc 60 stored in 10% NaCl solution between 1–28 days and 100% relative humidity atmosphere afterwards (150 day old samples)

Table 3

Weight loss of 1 day old hydrated cements calculated from TG curves of derivatograms

Sign	130 − 640 °C bound water %	20 − 130 °C water content %	640 − 750 °C CO_2 %	under 900 °C total %
1	6.82	10.00	1.77	18.59
2	6.66	7.75	1.53	15.94
3	6.74	11.45	1.50	19.69
4	6.78	8.63	1.21	16.62
5	4.27	5.41	2.25	11.93
6	4.60	9.09	1.70	15.39
7	4.41	6.98	1.53	12.92
8	−	−	−	−
9	5.61	9.81	1.47	16.89
10	4.38	8.13	2.00	14.51
11	4.09	6.65	2.47	13.21
12	3.69	11.39	1.54	16.62
13	4.94	12.00	1.16	18.10
14	4.06	9.77	1.63	15.46
15	4.52	7.88	1.75	14.15
16	3.93	3.51	1.50	8.94
17	7.36	7.86	1.17	16.39
18	2.90	10.43	1.96	15.29
19	3.16	4.85	2.19	10.20
20	3.39	6.68	2.11	12.18

DTG curves of cement samples stored in NaCl solution (10% concentration or saturated) between 1–28 days show peaks of reasonably increased intensity that belong to the water loss of AF_m phases (between 180 and 300 °C); even the division of the peak around 300 °C into partial peaks may be observed (*Fig. 3*). The appearance of the new component ($C_3A \cdot CaCl_2 \cdot H_{10}$) shown by X-ray diffraction analysis as well proves that chloride ion from outer source may also bind into cement constituents. Cement type S 54 350 pc which contains calcium-aluminate in the form of C_4AF forms the analogous $C_3F \cdot CaCl_2 \cdot H_{10}$ containing ferrite. Chloro-aluminate-hydrates form solid solutions with the present AF_m phases (C_4AH_{13}, $C_3A \cdot CaSO_4 \cdot H_{12}$ or occasionally $C_3A \cdot CaCO_3 \cdot H_{11}$) − though not always and not under any proportional ratios. This is another possible reason for the peaks to unite into one.

The derivatogram of samples stored in NaCl shows three more minima over the peak of portlandite (460 °C). The one at 580 − 630 °C belongs to the water desorption of C-S-H, the one at 750 °C originates from the sublimation of NaCl adsorbed to the surface of the samples. The peak around 680 − 720 °C is not surely connected to $CaCO_3$, as samples not

Table 4

Weight loss of 28 day old hydrated cements calculated from TG curves of derivatograms

Sign	130 − 640 °C bound water %	20 − 130 °C water content %	640 − 850 °C CO$_2$-NaCl %		under 900 °C total %
1	9.88	8.22	–	1.53	20.23
2	11.51	8.16	–	1.66	21.33
3	10.72	10.00	1.50	–	22.22
4	11.36	8.36	1.55	–	21.27
5	7.89	9.57	1.31	1.74	20.51
6	6.62	8.06	1.00	1.82	17.48
7	–	–	–	–	–
8	6.54	7.65	2.00	–	20.89*
9	7.46	9.27	1.40	1.35	19.48
10	6.71	10.14	1.44	1.77	20.06
11	8.15	8.25	2.06	–	18.46
12	7.41	9.13	1.76	–	18.30
13	8.54	10.77	0.60	0.77	20.68
14	6.58	6.73	1.17	1.00	15.45
15	9.01	6.18	3.46	–	18.65
16	6.27	4.81	2.43	–	13.51
17	11.36	9.41	1.80	–	22.57
18	6.66	6.92	1.29	–	19.27*
19	6.97	8.39	1.54	–	16.90
20	6.48	4.56	3.04	–	14.08

* = samples 8 and 18 are to be repeated

exposed to NaCl treatment show a DTG minimum for CaCO$_3$ approx. 30 °C higher.

As the X-ray diffractogram proved the appearance of only one single chloridous hydrate (the Friedel-salt), we cannot state that the DTG peak around 680 °C belongs to any of the chloridous phases.

The changes described above appeared only after the age of 56 days on the derivatogram of samples stored in 10% or concentrated NaCl solution between 28 and 56 days. This means that chloride ions may bind into already hardened concretes as well.

The DTG curves of samples of the different cement types hydrated under various conditions are shown in *Fig. 4* (450 Rpc), *Fig. 5* (S 54 350 pc), *Fig. 6* (350 ppc 20) and *Fig. 7* (250 kspc 60). The figures show that the difference between DTG curves of samples stored in 10% or concentrated NaCl solution is less than the differences shown by curves of a sample stored in a solution of the same concentration recorded at different ages. This means that the time and duration of the storage in salt solution has more

Table 5

Weight loss of 56 day old hydrated cements calculated from
TG curves of derivatograms

Sign	130 − 640 °C bound water %	20 − 130 °C water content %	640 − 850 °C CO$_2$-NaCl %		under 900 °C total %
1	11.12	10.10	−	1.47	22.69
2	9.37	8.82	−	2.36	20.55
3	11.13	19.45	1.20	0.67	22.45
4	10.60	8.33	−	1.81	20.74
5	7.06	7.35	2.03	1.35	17.79
6	8.61	9.18	1.00	1.67	20.46
7	6.73	9.12	1.75	0.88	18.48
8	5.22	7.35	1.62	1.56	15.75
9	7.73	9.52	1.34	1.32	19.91
10	7.98	10.00	1.00	1.50	20.48
11	8.80	8.55	1.72	0.83	19.90
12	7.71	8.72	1.47	0.70	18.60
13	10.41	8.53	1.77	1.01	21.72
14	11.98	7.65	0.92	1.40	21.95
15	9.94	9.40	0.72	0.88	20.94
16	7.69	6.39	0.68	0.67	15.13
17	11.68	10.25	1.50	−	23.43
18	5.62	7.05	3.41	−	16.08
19	8.24	9.35	1.94	−	19.53
20	7.47	7.53	2.35	−	17.35

influence on the composition of hydrate phases than the concentration of the NaCl solution.

Portlandite, ettringite, C_3S, βC_2S, C_4AF and $CaCO_3$ may be detected on all X-ray spectra for samples stored in an atmosphere of 100% relative humidity and saturated NaCl solution between 1–28 days (*Figs. 8* and *9*). The X-ray spectrum for the sample of 250 kspc 60 cement stored in 100% relative humidity atmosphere shows reflections in addition of C_3A, type 350 ppc 20 shows reflections of C_3A and quartz, while type 450 Rpc has reflections of C_3AH_6.

All samples stored in NaCl solution show reflections of $C_3A \cdot CaCl_2 \cdot H_{10}$, $C_4A \cdot H_{13}$ and their solid solutions. The ferrite containing analogue has the reflections for $C_3F \cdot CaCl_2 \cdot H_{10}$ at the same position as those of chloro-aluminate-hydrate. Most interestingly $C_3A \cdot CaSO_4 \cdot H_{12}$ cannot be detected on any of the spectra, though little low intensity reflections marking the presence of ettringite appear at each sample. This shows the low SO_4^{2-} concentration of the AF_m phase, or the level of crystallisation of monosulphate.

Table 6

Weight loss of 90 day old hydrated cements calculated from
TU curves of derivatograms

Sign	130 – 640 °C bound water %	20 – 130 °C water content %	640 – 850 °C CO$_2$-NaCl %		under 900 °C total %
1	1.29	7.87	–	3.25	2.41
2	11.17	7.06	2.77	3.65	24.58
3	10.81	5.82	2.58	2.39	21.60
4	11.17	8.23	1.76	2.64	23.80
5	7.72	7.93	2.06	1.61	19.32
6	9.68	9.44	1.21	1.45	21.78
7	9.66	10.01	1.92	1.15	22.74
8	9.08	8.98	1.46	1.17	20.69
9	10.45	9.85	1.55	1.43	23.28
10	9.05	9.12	1.18	1.24	20.59
11	10.91	9.75	2.06	0.59	23.51
12	10.45	10.62	2.08	0.64	23.79
13	9.39	9.65	1.25	0.79	21.08
14	10.58	10.05	1.00	0.88	22.51
15	12.61	10.56	1.41	1.00	25.58
16	10.25	7.81	1.29	0.71	20.06
17	11.90	9.82	2.50	–	24.22
18	8.11	7.65	3.42	–	19.18
19	9.06	10.19	2.80	–	22.05
20	7.70	7.55	2.36	–	17.61

The X-ray diffractograms do not show any reflections marking the formation of chloro-silicate-hydrate. Though reflections of tobermorite were observed only at the sample of 350 ppc 20 cement type but it is undoubtedly, that 'C-S-H gel' occurs in every sample.

4. Summary

1. Our experiments proved that C$_3$A · CaCl$_2$ · H$_{10}$ (Friedel-salt) appears even in hardened cement samples over the age of 28 days under the influence of NaCl solution. This means that NaCl used for wintertime defrostation may build in into already hardened concretes as well.
2. Both X-ray diffraction spectra and thermal analysis proved that the chloride of NaCl is bound by C$_3$A and C$_4$AF in the form of C$_3$A · CaCl$_2$ · H$_{10}$ and C$_3$F · CaCl$_2$ · H$_{10}$.

Table 7
Weight loss of 180 day old hydrated cements calculated from
TG curves of derivatograms

Sign	$130 - 640 \, ^\circ C$ bound water %	$20 - 130 \, ^\circ C$ water content %	$640 - 850 \, ^\circ C$ CO_2-NaCl %		under $900 \, ^\circ C$ total %
1	12.08	8.23	–	1.00	21.31
2	11.64	9.68	–	1.17	22.49
3	12.92	7.94	1.18	0.59	22.63
4	12.09	8.32	0.82	1.03	22.26
5	9.63	7.33	2.33	1.34	20.63
6	8.65	8.55	1.47	1.33	20.10
7	9.08	8.49	1.86	0.77	20.20
8	8.57	9.86	1.88	1.18	21.49
9	9.87	9.07	1.51	1.05	22.50
10	11.80	5.74	1.00	1.29	19.83
11	12.25	6.13	2.04	0.58	20.90
12	11.41	6.43	1.61	0.71	20.16
13	9.77	9.02	1.40	0.77	20.96
14	10.18	10.29	0.91	0.65	22.03
15	11.25	9.11	1.00	0.65	22.01
16	9.42	8.15	0.65	0.53	18.75
17	11.75	8.54	1.64	–	21.93
18	9.42	9.45	2.65	–	21.52
19	8.84	7.34	3.56	–	19.74
20	8.12	7.05	3.17	–	18.34

3. In case of cement pastes stored in NaCl solution at certain phases. of hydration the appearance of monosubstituted phases containing chloride was evident in all four cement types.

4. $C_3A \cdot CaCl_2 \cdot H_{10}$ may be formed from calcium-aluminate-hydrates in the initial phase of hydration or may be formed by the substitution of anions of AF_m phases ($C_3A \cdot CaSO_4 \cdot H_{12}$, $C_3F \cdot CaSO_4 \cdot H_{12}$, $C_3A \cdot CaCO_3 \cdot H_{11}$, $C_3F \cdot CaCO_3 \cdot H_{11}$) already present.

5. The amount of the generated $C_3A \cdot CaCl_2 \cdot H_{10}$ is determined mainly by the C_3A and C_4AF content of cements under a given NaCl concentration.

6. X-ray diffraction analysis did not show the appearance of calcium-silicate-hydrate containing chloride. Relevant literature has not yet served with proof whether chlorides 'tightly bound' by C-S-H gel are bound by chemical forces or not. Identification of the characteristics of chemical connections was impossible in these cases.

7. Hydraulic additives did not affect basic chemical connections significantly, chemical bonds were only detected with C_3A and C_4AF clink-

ers. Hydraulic additive materials influenced the absorption of chlorides instead.

Acknowledgement

References

1. RASHEEDUZZAFAR, EHTESHAM HUSSAN, S. – AL-SAADOUN, S. S. (1991): Effect of Cement Composition on Chloride Binding and Corrosion of Reinforcing Steel in Concrete. CCR, Vol. 21, pp. 777–794.
2. PAGE, C. L. – SHORT, N. R. – HOLDEN, W. R. (1986): The Influence of Different Cements on Chloride-Induced Corrosion of Reinforcing Steel. CCR, Vol. 16, pp. 79–86.
3. MONTEIRO, P. J. M. – GJORV, O. E. – MEHTA, P. K. (1985): Microstructure of the Steel-Cement Paste Interface in the Presence of Chloride. CCR, Vol. 15, pp. 781–784.
4. ODLER, I. – ABDUL-MAULA, S. (1984): Possibilities of Quantitative Determination of the AF_t (Ettringite and AF_m (Monosulphate) Phases in Hydrated Cement Pastes. CCR, Vol. 14, pp. 133–141.
5. KAYYALI, O. A. – HAQUE, M. N. (1988): Chloride Penetration and the Ratio of Cl^-/OH^- in the Pores of Cement Paste. CCR, Vol. 18, pp. 895–900.
6. PAGE, C. E. – VEENNESLAND, (1983): Pore Solution Composition and Chloride Binding Capacity of Silica-Fume Cement Pastes. Mater. Constr., Vol. 16, pp. 19–25.
7. MIDGLEY, H. G. – ILLSTON, J. M. (1984): The Penetration of Chlorides into Hardened Cement Pastes. CCR, Vol. 14, pp. 546–558.
8. ARYA, C. – BUENFOLD, N. R. – NEWMAN, J. B. (1990): Factors Influencing Chloride-Binding in Concrete. CCR, Vol. 20, pp. 291–300.
9. BEN-YAIR, M. (1974) : The Effect of Chlorides on Concrete in Hot and Acid Regions. CCR, Vol. 4, pp. 405–417.
10. BEAUDOIN, J. J. – RAMACHANDRAN, V. S. – FELDMAN, R. F. (1990): Interaction of Chloride and C-S-H. CCR, Vol. 20, pp. 875–883.
11. BALÁZS, GY. – CSIZMADIA, J. – KOVÁCS, K. (1996): Chloride Binding Ability of (Clinker Minerals) C_3A, C_4AF and C_3S. – In press.
12. TRITTHART, I. (1992): Changes in Pore Water Composition and in Total Chloride Content at Different Levels of Cement Paste Plates under Different Storage Conditions. CCR, Vol. 22, pp. 129–138.
13. TAYLOR, M. F. W. (1990): Cement Chemistry. Academic Press, London, p. 208.
14. BENSTED, J. – VARMA, S. P. (1974): Hydration of Portland Cement and its Constituents. Cem. Technol., Vol. 5, pp 440–450.